Oceanologia 64 (2022) 88—102

Available online at www.sciencedirect.com

ScienceDirect

journal homepage: www.journals.elsevier.com/oceanologia

ORIGINAL RESEARCH ARTICLE

Assessment of Sentinel-2 to monitor highly dynamic small water bodies: The case of Louro lagoon (Galicia, NW Spain)

Gema Casal*

National Centre for Geocomputation, Maynooth University, Maynooth, Co. Kildare, Ireland

Received 8 April 2021; accepted 17 September 2021
Available online 6 October 2021

KEYWORDS
Coastal lagoons;
Intermittent inlet;
Water bodies;
Coastal monitoring;
Multiband water indices

Abstract Coastal lagoons have been providing ecological, economic and cultural benefits for many centuries. Despite their importance, the monitoring of coastal lagoons poses numerous challenges related to their complex environmental processes, their large variability in size and their remote location, inhibiting effective management programmes. This study demonstrates the effectiveness of Sentinel-2 satellites to map highly dynamic morphological and hydrological changes in the Louro lagoon, a small choked lagoon located on the Galician coast (NW Spain). For this purpose, a simple methodology using the Normalised Difference Water Index (NDWI) has been evaluated, which allows to monitor the sand barrier changes and the inlet formation. The results show that the sand barrier's opening and closing might take only a very short period, and the recovery of the lagoon to its full water level can happen in less than a month. Sentinel-2 images also reveal drastic changes in the water level once the sand barrier is broken. A water surface area of 0.24 km^2 was estimated on 04/11/2019, while this surface was reduced to 0.10 km^2 on 04/12/2019. Monitoring these changes is critical to understand the different processes

* Corresponding author at: National Centre for Geocomputation, Maynooth University, Maynooth, Co. Kildare, Ireland.
E-mail address: gema.casal@mu.ie

Peer review under the responsibility of the Institute of Oceanology of the Polish Academy of Sciences.

Production and hosting by Elsevier

https://doi.org/10.1016/j.oceano.2021.09.004

ongoing in these valuable environments and making informed decisions for their management and protection.

1. Introduction

Coastal lagoons occupy 13% of the global coastline (Barnes, 1980; Kjerfve, 1994) and represent essential ecosystems that provide many ecological, economic, social and cultural benefits. Several definitions for coastal lagoons have been proposed (Tagliapietra et al., 2009). The most widely used is the one suggested by Kjerfve (1994) that define coastal lagoons as "a shallow coastal water body separated from the ocean by a barrier, connected at least intermittently by one or more restricted inlets and usually oriented shore-parallel". Bird et al. (1994) added to this definition some aspects regarding the enclosing barrier whose nature is responsible for lagoon formation (Duck and Figueiredo da Silva, 2012). These authors define coastal lagoons as "areas of relatively shallow water that have been partly or wholly sealed off from the sea by the deposition of spits or barriers, usually of sand or shingle, build up above high tide level by wave action". Considering their geomorphology and degree of isolation coastal lagoons can be sub-divided into: "chocked", "restricted" and "leaky" (Kjerfve, 1994). Following Kjerfve (1994) "chocked" lagoons are connected to the sea by a single long narrow entrance channel and usually located along a stretch of coast with high wave energy and significant littoral drift; "restricted" lagoons consist of a large and wide water body, usually oriented parallel to the coast, with two or more entrance channels, while "leaky" lagoons are elongated water bodies parallel to the coast but with many ocean entrance channels.

Coastal lagoons are highly variable systems influenced both by global aspects such as climate change or sea-level rise and by local aspects such as the nature of the basement, coastal orientation, topography or sediment sources (Costas et al., 2009). The local aspects have particular relevance on the NW Iberian coast, which has an abrupt topography with incised river valleys, producing shallow and small coastal lagoons (<1 km^2 in size) (González-Villanueva et al., 2015). In Galicia (NW Spain), these small coastal lagoons are relevant environments that provide many ecosystem services and that are protected by the "Habitat Directive of the European Union" (92/43/EEC) (EC, 1992). A large number of these lagoons holds protected taxa, some of which are listed in the "Galician Catalogue of Endangered Species" (González-Villanueva et al., 2015).

Despite the current environmental protection of Galician coastal lagoons, these systems are progressing towards their collapse (Fraga-Santiago et al., 2019). The principal observed cause is clogging (accumulation of sediment particles), which leads the free water body to disappear, implying a progressive loss of diversity, mainly of aquatic birds (Bao et al., 2007). This effect is of particular relevance in the Louro lagoon. As a choked lagoon, the Louro lagoon has shallow waters periodically connected with the open ocean by a narrow channel (called an inlet). The temporary connection between the lagoon and the open sea causes significant hydrodynamic variations. This change is probably the most critical factor governing the structure and functioning of the resident biotic communities (Smakhtin, 2004). In many choked lagoons, the occasional break of the sand barrier might be produced in an artisanal manner associated with cultural traditions, generally related to fisheries (Bertotti-Crippa et al., 2013) or agricultural purposes (Fortunato et al., 2014). In the case of the Louro lagoon, due to the abandonment of traditional agriculture practises, the sand barrier's opening mainly depends now on meteorological and oceanographic conditions.

In choked lagoons, the opening of the sand barrier has a direct effect on their morphology and biogeochemical flows by promoting the exchange of water, sediments, nutrients, and pollutants between the lagoon and the sea (Moreno et al., 2010). After the rupture, the sand barrier can remain open or close after a variable period of time, depending on the hydraulic efficiency related to the rainfall regime, the tide cycle and the sediment transport at the local level (Green et al., 2013). These openings can occur regularly throughout the year (seasonal cycles) or irregularly due to anthropogenic interventions. For example, seasonal openings can be caused by high waves produced by storms, intense river discharges, or elevated rain levels (Gale et al., 2006; Weidman and Ebert, 2013). The unpredictable nature of natural closures and openings hampers their monitoring and, in many cases, they have not been explicitly evaluated (Yáñez-Aranciabia et al., 2014). Information about the evolution of coastal lagoons and their monitoring is crucial for their management and sustainable protection (Newton et al., 2018). However, the environmental and morphological variability, together with their isolation and dispersion, makes it challenging to acquire robust and continuous data of coastal lagoons, and thus to establish a holistic management approach. On the other hand, there is a growing need to expand the coverage and frequency of coastal monitoring for regulation purposes, which derive from legislation such as the European Union Water Framework Directive (WFD) (2000/60/EC) (EC, 2000). The WFD considers coastal lagoons as both "transition waters" and "coastal waters" that need specific monitoring instruments to assess their ecological status and derive possible actions.

Data obtained by remote sensors, combined with in situ monitoring programmes, are crucial to provide new knowledge of the diverse processes taking place in coastal lagoons. The use of satellite data is well established in different applications related to coastal water bodies such as flood monitoring (DeVries et al., 2020), water quality assessment (Gholizadeh et al., 2016) or the extraction of surface water area (Sun et al., 2012). In light of increasing new satellite data, the present moment is particularly impor-

tant to provide new knowledge in this field. As part of the Copernicus programme, the European Space Agency (ESA) together with the European Commission has launched the Sentinel missions to increase existing Earth observation capabilities. Of particular relevance for the study and monitoring of coastal areas is the Sentinel-2 mission. This mission includes the twin satellites Sentinel-2A, launched in 2015, and Sentinel-2B, launched in 2017. The Multispectral Imager (MSI) sensor on board Sentinel-2 provides 13 spectral bands covering from visible and near-infrared (VNIR) to shortwave infrared (SWIR) wavelengths, with four of these bands (B2, B3, B4 and B8) offering a spatial resolution of 10 m. This relatively high spatial resolution combined with a short revisit time (5 days at the equator and 2—3 days at mid-latitudes) is an advantage for monitoring highly dynamic small water bodies. Sentinel-2 data will have a temporal continuity with the launch of Sentinel-2C and Sentinel-2D in the future.

Although the Sentinel-2 satellites were primarily designed for terrestrial environments, numerous studies have shown their usefulness for different coastal applications (e.g. Ansper and Alikas, 2019; Casal et al., 2020; Hedley et al., 2018), including coastal lagoons (Brisset et al., 2021; Sebastiá-Frasquet et al., 2019) and water bodies delimitation (Zhou et al., 2017). Sentinel-2 provides continuity regarding medium resolution missions such as Satellite Pour l'Observation de la Terre (SPOT) or Landsat, which have provided successful results in the mapping of diverse water bodies (Casal et al., 2011; Lavery et al., 1993; Luis et al., 2019). The Landsat mission had been used extensively due to its open data access and long-term data series (the first Landsat satellite was launched in the 70s). However, the revisit time of Landsat satellites (16 days) limits their use for monitoring highly dynamic events.

Regarding coastal lagoons, the number of studies using Sentinel-2 data is still scarce. A search in the Web of Science using the words "Sentinel-2" and "lagoon" as topic reported only 17 records between 2017 and 2020, including articles and proceeding papers. The Sentinel-2 applications in coastal lagoons mainly include monitoring water quality parameters (Braga et al., 2020; Sebastiá-Frasquetet al., 2019; Sòria-Perpinyà et al., 2020) and only a few applications were found related to water body changes (Karim et al., 2019) and waterline detection (Salameh et al., 2020). None of the records reported by Web of Science included highly dynamic changes.

The objective of this study is the evaluation of Sentinel-2 data to monitor highly dynamic morphological and hydrological changes in a small chocked lagoon. The detection of the breaking and closing of the sand barrier, the inlet formation and the water level variations are assessed using existing water extraction indices. Establishing the barrier break frequency and its closure is crucial for evaluating the barrier vulnerability and preventing damage to infrastructures and ecosystem services.

2. Material and methods

2.1. Study area

The Louro lagoon is located on the Atlantic coast of Galicia (NW Spain) at the northern end of the Ría de Muros (Figure 1). This area, catalogued as a "Site of Community Importance" (Natura 2000 Network, Directive 92/43/EEC) under the European Union Habitats Directive, is an essential habitat for many species of fauna and flora (González-Villanueva et al., 2017). The lagoon ecosystem hosts amphibians, reptiles and small mammals and has become a relevant place for ornithological observation.

The Louro lagoon is separated from the open sea by a sand barrier of 300—600 m wide and 1500 m long, fixed to a rocky substrate on both sides (González-Villanueva et al., 2017). The sand barrier hosts vegetated dunes fragmented by corridors produced by wind action. The lagoon is mainly shallow, with depths ranging between 2 m in winter and 0.5 m in summer (Pérez-Arlucea et al., 2011). It presents an inner permanent flood area and a peripheral area subject to occasional flood periods (Pérez-Arlucea et al., 2011). Precipitation in the study area is highly variable, with oscillations between monthly averages of 300 mm in autumn-winter to less than 50 mm in summer. Communication between the lagoon and the open sea is temporary and occurs under certain circumstances related to spring tides, intense rain periods and storms with south-southwesterly winds. The sand barrier break causes a water exchange between the open sea and the lagoon through the formation of an inlet. In general, the inlet can be described as a channel 2 m deep and an average of 15 m wide that cuts the barrier perpendicular to the coast (González-Villanueva et al., 2013; Pérez-Arlucea et al., 2011). The Louro lagoon system is classified as mesotidal (Davies, 1964), with an average tidal range of around 3 m.

Recent studies have demonstrated that the Louro lagoon is experiencing a progressive siltation and eutrophication process, which alters its natural evolution and could eventually affect its inherent environmental value (González-Villanueva et al., 2015; Fraga-Santiago et al., 2019). Several factors have been identified affecting these processes, the most relevant of which is the abandonment of traditional agriculture practices (Fraga-Santiago et al., 2019) that lead to changes in the land use around the lagoon. Since the last decades of the 20th century, crop cultivation has been progressively abandoned, leading to riparian forest growth (Fraga-Santiago et al., 2019). This expansion in tree-covered areas around the lagoon implied a decrease in water availability. Moreover, frequent forest fires have also contributed to transporting nutrients and sediments into the lagoon, thus incrementing the siltation and eutrophication processes.

2.2. Satellite imagery

The intense storms in winter 2019/2020 severely impacted the Louro lagoon by producing several breaks of the sand barrier with the subsequent formation of an inlet. Prior information about morphological and environmental changes in the Louro lagoon during this period motivate this study to evaluate the suitability of Sentinel-2 images to monitor these processes. Sentinel-2 images were downloaded from the Copernicus Scientific Data Hub between 1st November 2019 and 29th February 2020 at level 1C, Top-of-Atmosphere reflectance (TOA) and projection UTM/WGS84.

Although a total number of 24 Sentinel-2 images were registered during this period, only seven had no clouds or

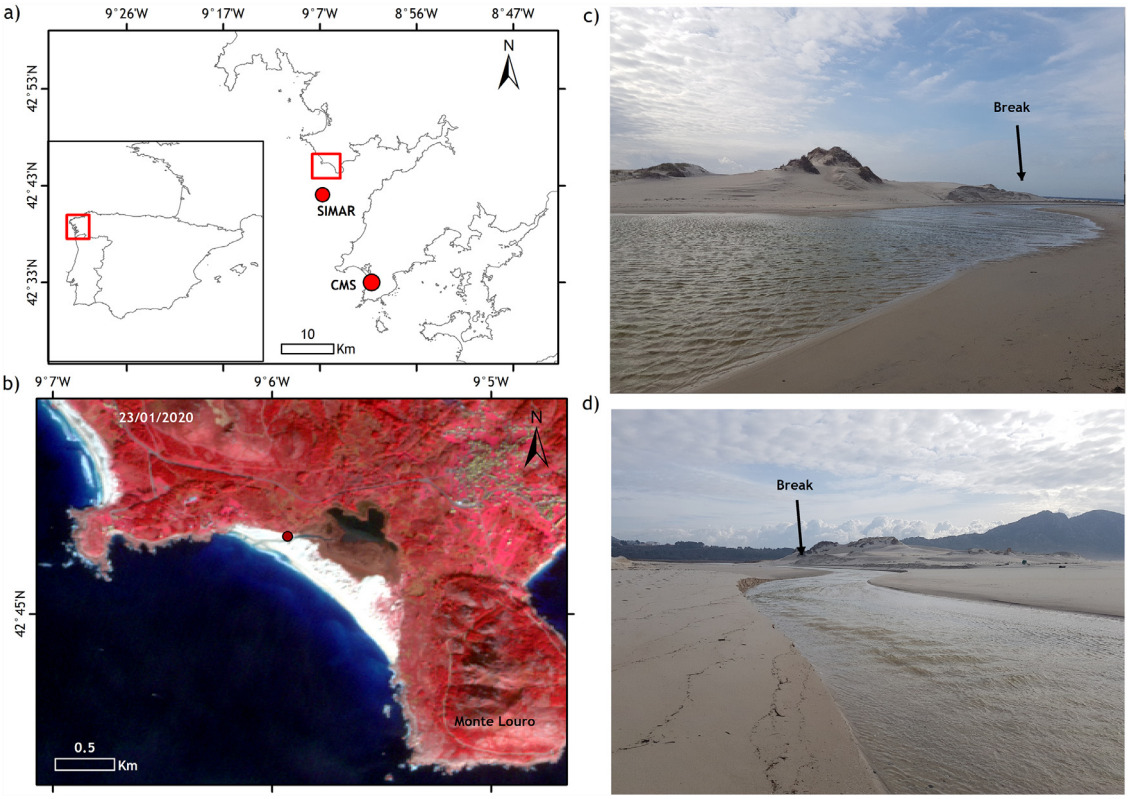

Figure 1 a) Map of the study area showing the locations of the SIMAR node and the Corrubedo Meteorological Station (CMS). b) Sentinel-2 image in false infrared colour (NIR, R, G), taken on 23/01/2020. This image also shows the sand barrier break . The red dot in b) indicates the place where the photographs in panels c) and d) were taken on 26/01/2020.

Table 1 Detail of the Sentinel-2 images included in the study. The tidal coefficient was registered in Muros Port and indicates the tidal amplitude (difference between low and high tide).

Date	Sensor	S2-granule	Acquisition time (UTM)	Tidal coefficient	Observations
04/11/2019	S2A	T29THM	11:33:21	34 (very low)	Strong swell
29/11/2019	S2B	T29THM	11:33:29	75 (high)	Clouds partially covering the lagoon
04/12/2019	S2A	T29THM	11:34:41	39 (low)	Strong swell
29/12/2019	S2B	T29THM	11:33:59	70 (high)	Strong swell
03/01/2020	S2A	T29THM	11:34:51	42 (low)	Clouds partially covering the lagoon
23/01/2020	S2A	T29THM	11:33:51	77 (high)	No swell. Low clouds over the open sea but not over the actual lagoon
22/02/2020	S2A	T29THM	11:33:11	44 (low)	Strong swell. Clouds over the open sea but not over the lagoon

a low cloud coverage (Table 1). Cloud coverage is a critical limiting factor in the NW of Iberian Peninsula; however, the revisit time of Sentinel-2 constellation allowed for at least two suitable images almost every month during the study period. Most of the images showed a strong swell with waves breaking in the shore producing white caps. No sun glint conditions were visually appreciated in any of the images. The images were resized to the area of the Louro lagoon.

2.3. Meteorological and oceanographic data

Because the break of the sand barrier in winter is mainly related to meteorological and oceanographic conditions, information about rainfall, wind and significant wave height was consulted for the period of this study (Figure 2). Rainfall data (L/m^2) and wind speed (km/h) were downloaded from the Corrubedo Meteorological Station (CMS) through the Meteogalicia website (https://www.meteogalicia.gal).

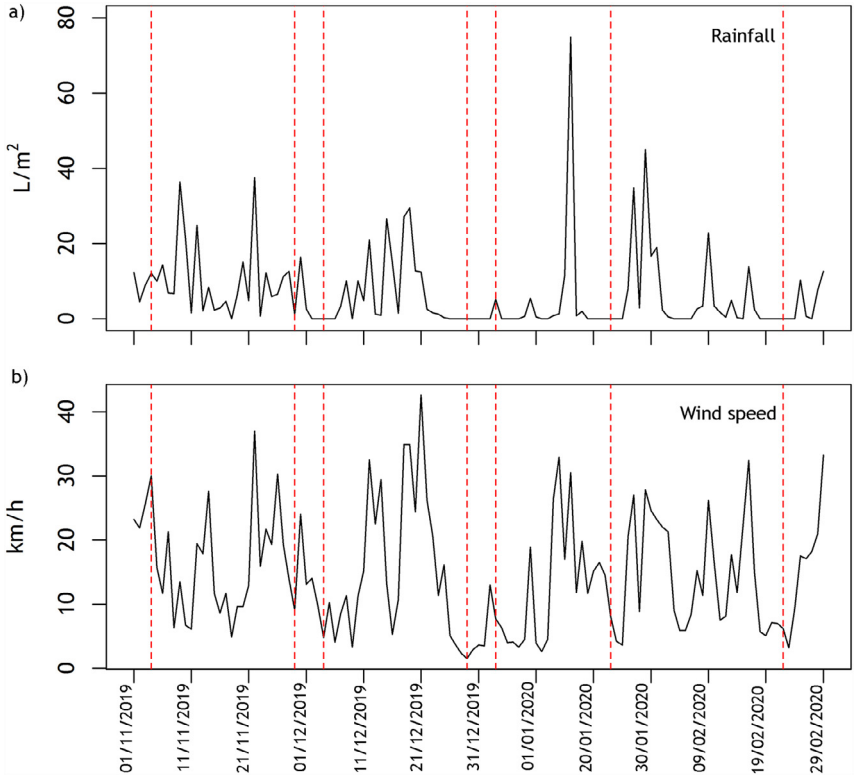

Figure 2 a) Daily rainfall data (L/m^2) and (b) wind speed (km/h) registered by the Corrubedo Meteorological Station. Red dashed lines indicate the dates on which the Sentinel-2 images analysed in this study were taken (Table 1).

The wave height was taken from the node of 3009017 of the SIMAR dataset provided by Puertos del Estado (http://www.puertos.es) (not shown here as the data are not downloadable). Numbers in the SIMAR database are obtained through a wave reanalysis model. The location of CMS and SIMAR node is shown in Figure 1.

2.4. Surface water delimitation

The extraction of water bodies from optical images uses the difference between the low reflectance levels of water surfaces and the high reflectance levels of terrestrial substrates in the infrared channels. Several algorithms for surface water delimitation have been proposed. Examples are the digitalisation of water bodies through visual interpretation (Yang et al., 2017), object-based image analysis (Zhang et al., 2013), spectral mixture analysis (Guo et al., 2015; Liu et al., 2017), single-band thresholding (Bryant and Rainey, 2002; Frazier and Page, 2000) or spectral water indices (Feyisa et al., 2014; McFeeters, 1996; Xu, 2006). The spectral water indices commonly take two different bands to distinguish the water surfaces, having the advantage of both simplicity and high precision (Xie et al., 2014). For this reason, these indices are among the most widely used.

One of the most popular multiband spectral water indices is the so-called Normalised Difference Water Index (NDWI) which uses the green and the near-infrared bands (McFeeters, 1996). The NDWI had first been developed using Landsat Multispectral Scanner images in digital numbers and a zero threshold value. Positive NDWI values were identified as water, while negative values were classified as non-water. Some years later, Xu (2006) proposed a different index, the Modified Normalized Difference Water Index (MNDWI), in which the green and shortwave infrared bands were used. Although the MNDWI is widely used in applications such as the delimitation of surface water bodies, land-use changes and ecology (Duan and Bastiaanssen, 2013; Xu, 2006), it has limitations in urban and shaded mountainous areas (Acharya et al., 2018). Some years later, Feyisa et al. (2014) proposed the Automated Water Extraction Index (AWEI) using Landsat Thematic Mapper. In this case, Feyisa et al. developed two variants: the AWEIsh designed to identify water bodies by eliminating shadow pixels and the AWEInsh designed to delimit water bodies in urban areas. Because the Louro lagoon area is a rural area without large urban settlements, the AWEInsh index was not considered here. The Normalised Difference Vegetation Index (NDVI) was also evaluated since several studies have demonstrated that vegetation indices can also be effective in delimiting water bodies (Rokni et al., 2014).

Most of the indices considered here were initially developed for satellites other than Sentinel-2. For this reason, their equations were adapted to Sentinel-2 bands as detailed in Table 2. This band adaptation approach is not novel and has already been described in other studies (Du et al., 2016; Wang et al., 2018; Yang et al., 2017). The selected Sentinel-2 bands were: band 2 (490 nm) as a blue band, band 3 (560 nm) as a green band, band 4 (665 nm) as

Table 2 Water surface extraction indices were considered in this study. ρ represents the top of atmosphere reflectance (TOA) at different Sentinel-2 bands.

Multiband Index	Equation	Water value	Reference
Normalised Difference Vegetation Index	NDVI= $(\rho_{B8} - \rho_{B4})/(\rho_{B8} + \rho_{B4})$	Negative	Rouse et al. (1973)
Normalised Difference Water Index	NDWI= $(\rho_{B3} - \rho_{B8})/(\rho_{B3} + \rho_{B8})$	Positive	McFeeters et al. (1996)
Modified Normalised Difference Water Index	MNDWI= $(\rho_{B3} - \rho_{B11})/(\rho_{B3} + \rho_{B11})$	Positive	Xu et al. (2006)
Automated Water Extraction Index	AWEIsh= $\rho_{B2} + 2.5^{*}\rho_{B3} - 1.5^{*}(\rho_{B8} + \rho_{B11}) - 0.25^{*}\rho_{B12}$	Positive	Feyisa et al. (2014)

a red band and band 8 (842 nm) as NIR band. Band 11 (1614 nm) and band 12 (2190 nm) were chosen for SWIR1 and SWIR2, respectively. All selected bands have a spatial resolution of 10 m except for SWIR1 and SWIR2 for which the resolution is 20 m per pixel. Image sharpening processes to convert 20 m bands into 10 m bands were not performed since this study aimed to develop a methodology as simple as possible so that potential users can implement it quickly. The SNAP 8.0 software was used to resample the bands with 20 m of spatial resolution into 10 m. The same software was also used for the generation of the indices.

All the water indices described above allow water pixels to be classified by applying a simple threshold (T), which can be adjusted to different images or different classification priorities. The determination of the optimal threshold value is of great importance for the accurate delimitation of water bodies, and it can be done manually (Meng et al., 2013; Xu et al., 2005) or using automated methods (Ji et al., 2009; Zhang et al., 2018). In this study, the threshold values (T) were initially set to zero but generally, threshold adjustments to individual situations can achieve a more accurate delineation of water bodies (Du et al., 2012; Sekertekin, 2019). The extracted water bodies were converted to polygons and water level changes were evaluated using ArcGIS 10.3.1.

3. Results

3.1. Selection of the optimal multiband indices

The performance of the different indices mentioned in Table 2 was first interpreted visually and compared with the near-infrared (NIR) band at 842 nm. NIR wavelengths are strongly absorbed by water and reflected by terrestrial vegetation and dry soil (Sun et al., 2012). Even though NIR bands can also be used to extract water bodies using a threshold, this process requires an individual evaluation in each image. Changes in the image conditions (e.g. illumination) can modify the optimal threshold value. These changes are minimised using band ratios; for this reason, the NIR bands were only used to support the interpretation results.

All the evaluated indices have a spatial resolution of 10 m; however, some bands used for the MNDWI and AWEIsh indices were resampled from 20 m to 10 m. It is also important to remind here that the Louro lagoon is located in a rural environment with small and isolated settlements in the surrounding areas. The terrain elevations of nearby Monte Louro (~241 m) produces shadows, but they do not affect the lagoon area. Taking into account these aspects, some differences were found between the indices in the visual analysis.

As expected, the lagoon's delimitation and its inlet were less defined when the indices with the 20 m bands, MNDWI and AWEIsh, were used (see Figure 3). The AWEIsh index results were more affected by the swell, and showed the highest values close to the shore where the waves were breaking. This issue was not evident in MNDWI, but this index seems to be more sensitive to the shade produced by terrain elevations (Figure 3). In this case, the shade does not affect the lagoon, but the 20 m bands lead to a lower definition at which the water surface and inlet were mapped. The NNDWI and the AWEIsh indices were excluded from the analysis to avoid adding a sharpening step to the processing chain.

The visual analysis of the NDVI and NDWI indices showed a clear differentiation between land and water and a better delimitation of the inlet because of the higher spatial resolution (10 m) (Figure 3). NDVI was initially developed for separating green vegetation from other surfaces. However, some studies reported that the NDVI performs well for water detection (Rokni et al., 2014), giving water features negative values. On the other hand, the NDWI enhances information about water bodies by including the green band while reducing vegetation and soil features (Li et al., 2013). The NDWI index classifies water features with positive values, while vegetation and soil are classified with negative values (McFeeters et al., 1996).

To evaluate the results obtained with NDVI and NDWI indices in more detail, the frequency density histograms were analysed. The differentiation between land and water pixels was confirmed by the density distributions (Figure 4). The histogram of both indices showed a clear bimodal distribution with a higher peak representing water pixels and a lower peak representing land pixels. In the NDWI the land and water peaks were further apart, indicating a better differentiation between both substrates. This behaviour was

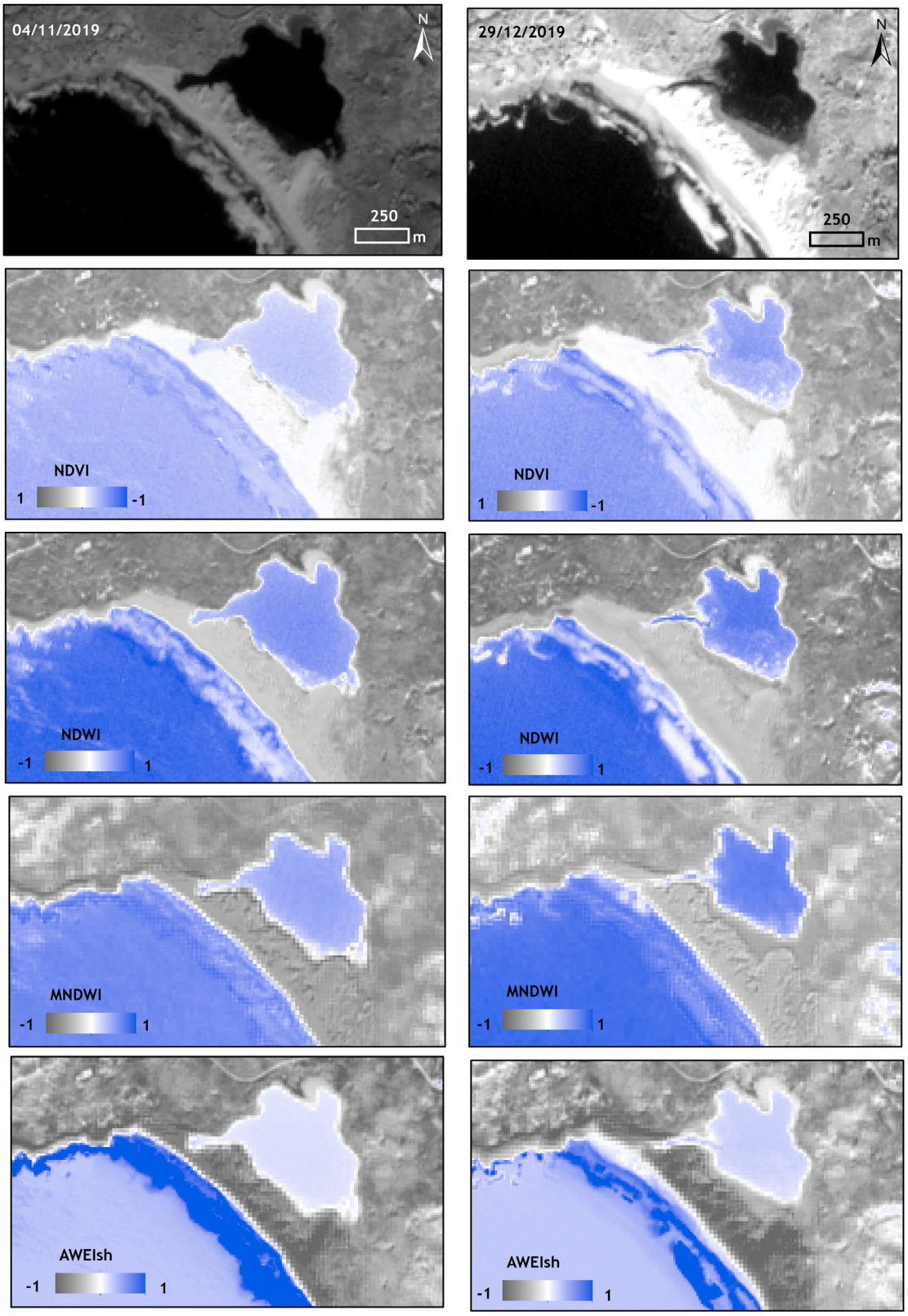

Figure 3 Example of the water surface extraction indices evaluated in this study applied to two different Sentinel-2 images (04/11/2019 and 29/12/2019). The first image on the left and right corresponds to band 8 (842 nm). The AWEIsh index values were rescaled to values between −1 and 1 for comparison with the other indices.

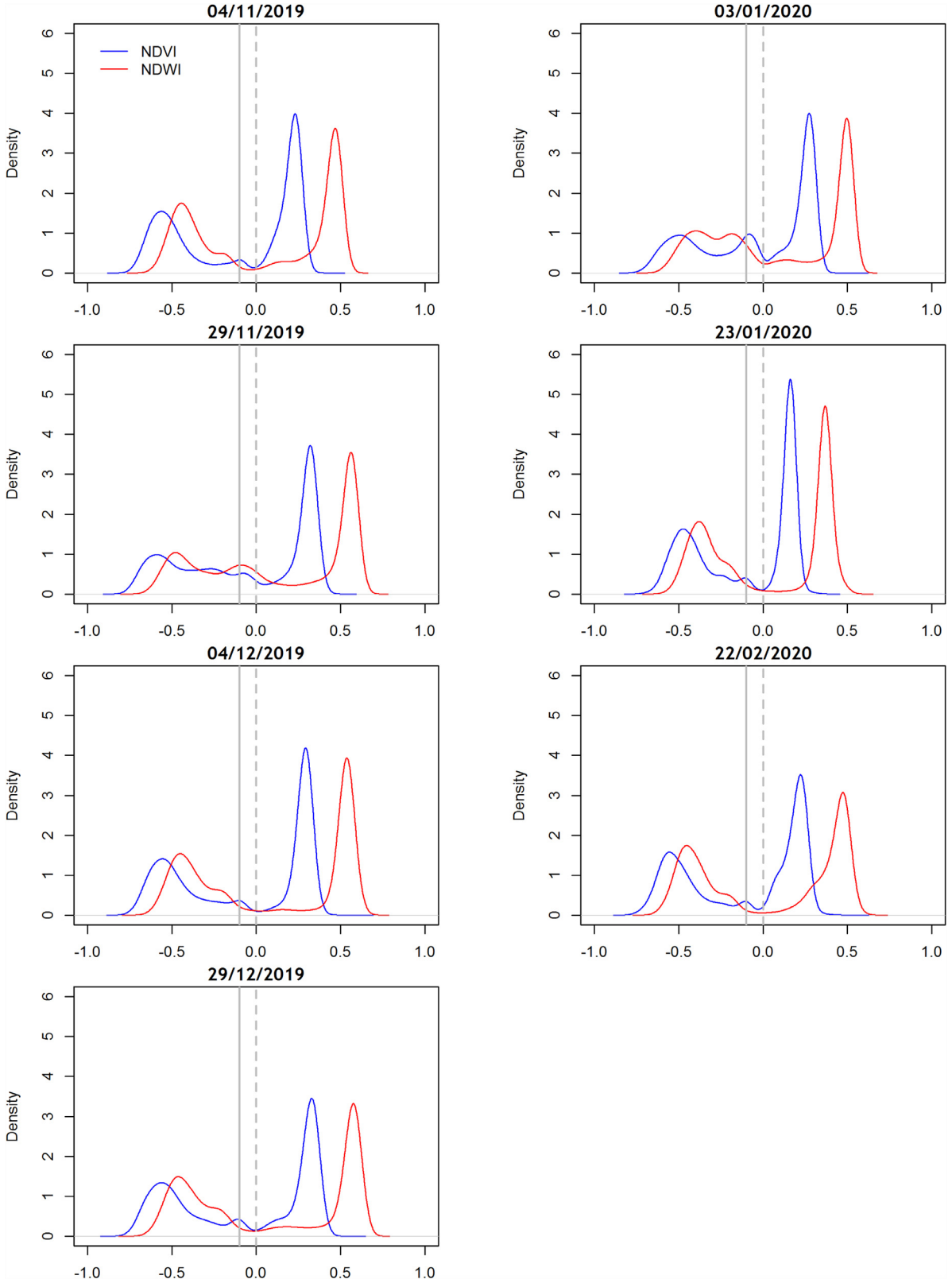

Figure 4 Density distributions of the NDVI and NDWI. The grey dashed line indicates the threshold value $T \geq 0$, while the solid line indicates a threshold of $T \geq -0.1$. NDVI values were inverted for a better comparison.

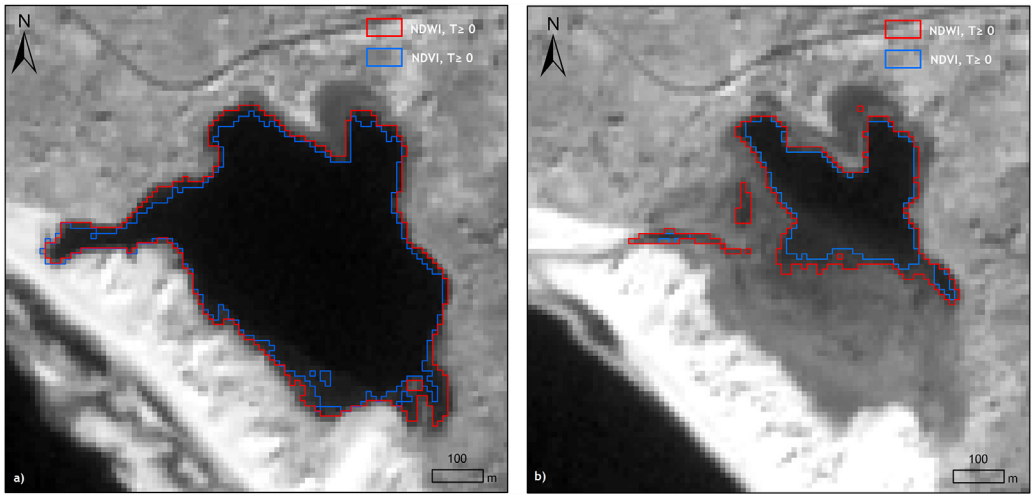

Figure 5 Comparison of the water surface extension using the NDVI and NDWI and a threshold value of $T \geq 0$. a) Delimitation of the water body on 04/11/2019. b) Delimitation of the water body on 23/01/2020. The NDVI shows more conservative results missing water pixels located at the edge of the lagoon.

confirmed by comparing the extracted water surface obtained by the two indices using the default threshold value of $T \geq 0$ (Figure 5). In all the cases, the NDVI showed more conservative results missing water pixels located on the water body's edge. This fact was especially evident when the lagoon showed a low water level, as was the case on 23/01/2020 (Figure 5b). For this reason, the NDWI was selected as the optimal index.

3.2. Delimitation of water surface

The histograms of the NDWI index showed a well-defined region between water and land peaks that could be interpreted as mixed pixels (Figure 4). Mixed pixels are caused by two or more land-cover classes in a surface area smaller than the spatial resolution of the image (Ji et al., 2009), and their amount will depend on the heterogeneity of the substrates. These mixed pixels can be identified in the histograms as a flat area between water and land peaks. Except for the images affected by clouds (29/11/2019 and 03/01/2020) the histograms revealed that mixed pixels could reach thresholds of −0.1 (Figure 4). Each image was individually evaluated in order to identify those pixels with a value lower than zero and higher than −0.1. All those pixels were located in well-defined areas at the lagoon's border. Further analysis is required since these pixels could be interpreted as pixels with a high water content but not submerged and pixels located in very shallow areas. When the lagoon had a high water level, both threshold values showed very similar results (Figure 6a); however, the largest differences were found when the water level started to decrease. In this case, a threshold value of $T \geq 0$ seems to be more conservative. This issue affects the inlet's delimitation since during the process of the sand barrier closing the water flow might be only a few centimetres deep (e.g. Figure 1b and 1c), and in this case, its delimitation using a threshold of $T \geq 0$ can be more challenging. Considering the objective of this study, the threshold value of $T \geq 0$ was selected. This value led to a good delimitation of the surface water level and allowed the inlet's detection and monitoring. For a more detailed delimitation of the inlet, further research would be required exploring other threshold values with the support of specific field campaigns.

Using a value of $T \geq 0$, the NDWI index was evaluated for the detection of the sand barrier break and its associated water level variations (Figure 7). The analysis of these Sentinel-2 images revealed that the Louro lagoon suffers significant morphological and hydrological variations. Between November 2011 and February 2020, the sand barrier broke and closed several times, allowing the water inside the lagoon to flow into the sea. The image acquired on 04/11/2019 showed the lagoon to have a high water level with the water about to flow over the dune crest. This situation presents a critical moment and indicates an imminent break of the sand barrier if the trigger conditions appear (e.g. heavy rains, southwesterly winds or high tides). During the storms, waves driven in the SW direction generate dissipative morphologies in the sand barrier and modify currents and sediment transport (Amécija et al., 2009). The current convergence promotes a rip current formation and the breaking of the sand barrier. However, the formation of the inlet and the consequent water outflow also needs the water elevation in the lagoon to be higher than the high tide water level by about 1 m, which requires prolonged periods of high rainfall levels (Pérez-Arlucea et al., 2011). This high water level generates enough pressure and potential energy to break the sand barrier, thus forming the inlet.

Between 04/11/2019 and 29/11/2019 meteorological data registered at the CMS weather station reported winds close to 30 km/h (Figure 2) while the SIMAR node showed significant wave heights (∼6 m). Moreover, between 09/11/2019 and 15/11/2019, the tide reached high coefficient values between 74 and 87. Meteorological factors, together with tides, could be the main triggers for breaking the sand barrier and forming the inlet detected on 29/11/2019. This Sentinel-2 image reveals that the inlet formation could have been produced some days before the image acquisition. This is suggested by the fact that the inlet shows a narrow part (Figure 7b), indicating that sand

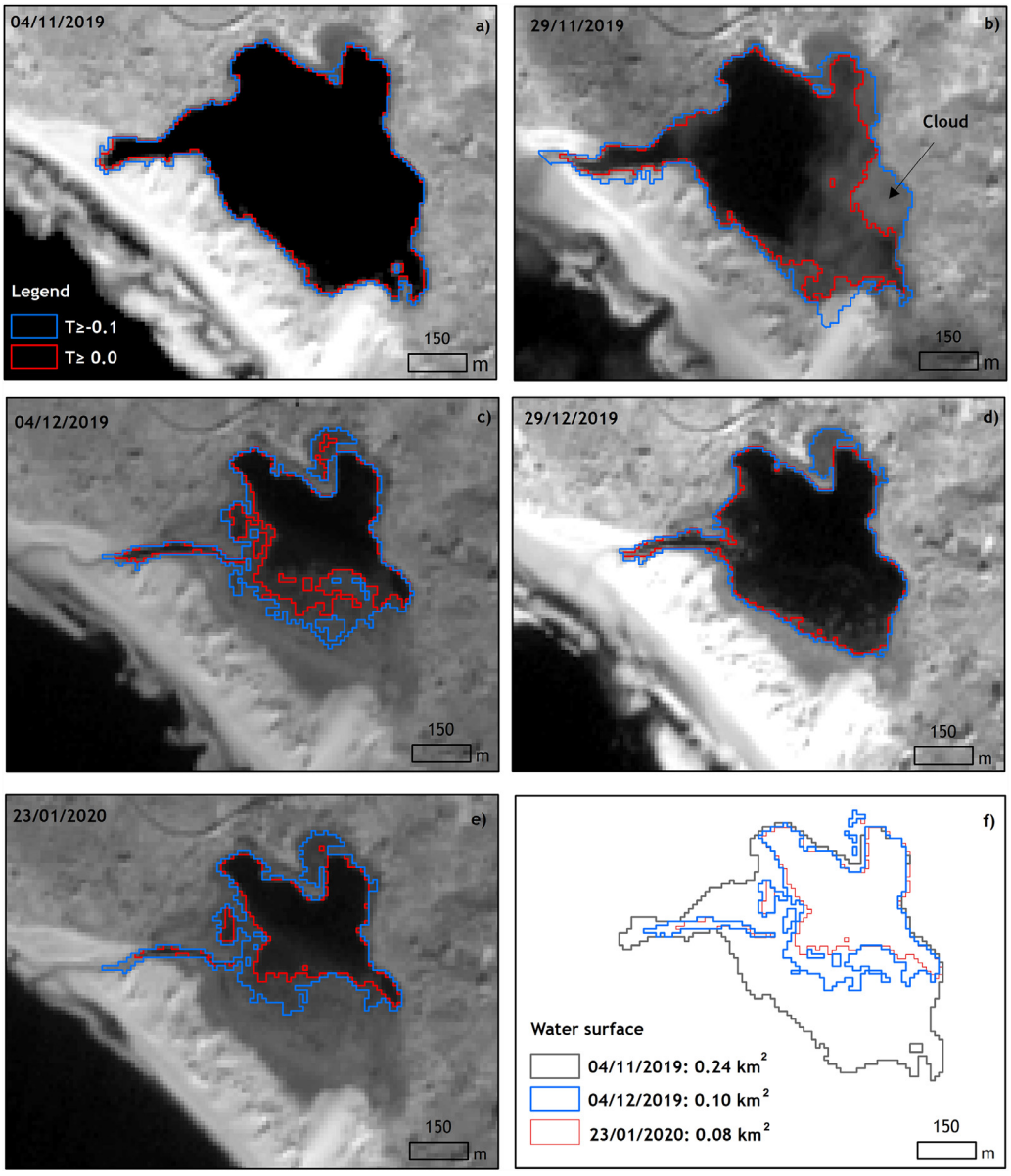

Figure 6 a—e) Example of extracted water body surfaces in different images using threshold values of $T \geq 0$ (red) and $T \geq -0.1$ (blue); f) variation of water levels using the NDWI and $T \geq 0$.

movements have already occurred and the communication with the open sea has started to reduce. The next available Sentinel-2 image, registered one month later (29/12/2019), showed the sand barrier sealed and the water level almost fully recovered. The Sentinel-2 image registered on 23/01/2020 revealed a lower water level again, indicating that a new break of the sand barrier had happened prior to the acquisition of the image. A heavy rain period (>70 L/m^2) in mid-January, together with moderate winds (~30 km/h) and high tide coefficients (74—92), could have triggered the inlet formation after 03/01/2013 since on this date the lagoon showed a high water level. The image registered on 22/02/2020 indicates a recovery of the sand barrier and the lagoon water level.

These observations confirm that the Sentinel-2 images showed the sand barrier to break and close several times during the four-month period. These changes were associated with meteorological and oceanographic conditions that produced drastic water level changes. During the timescale of only one month, the water surface can be reduced from 0.24 km^2 to 0.10 km^2 or even lower (Figure 6f). However, in wintertime and in the absence of breaks, the lagoon's water level can be fully recovered within less than a month.

4. Discussion

The results obtained in this study demonstrate that Sentinel-2 data can provide valuable information to detect and monitor highly dynamic morphological and hydrological changes in small coastal lagoons using a simple processing chain. This information can be essential to complement

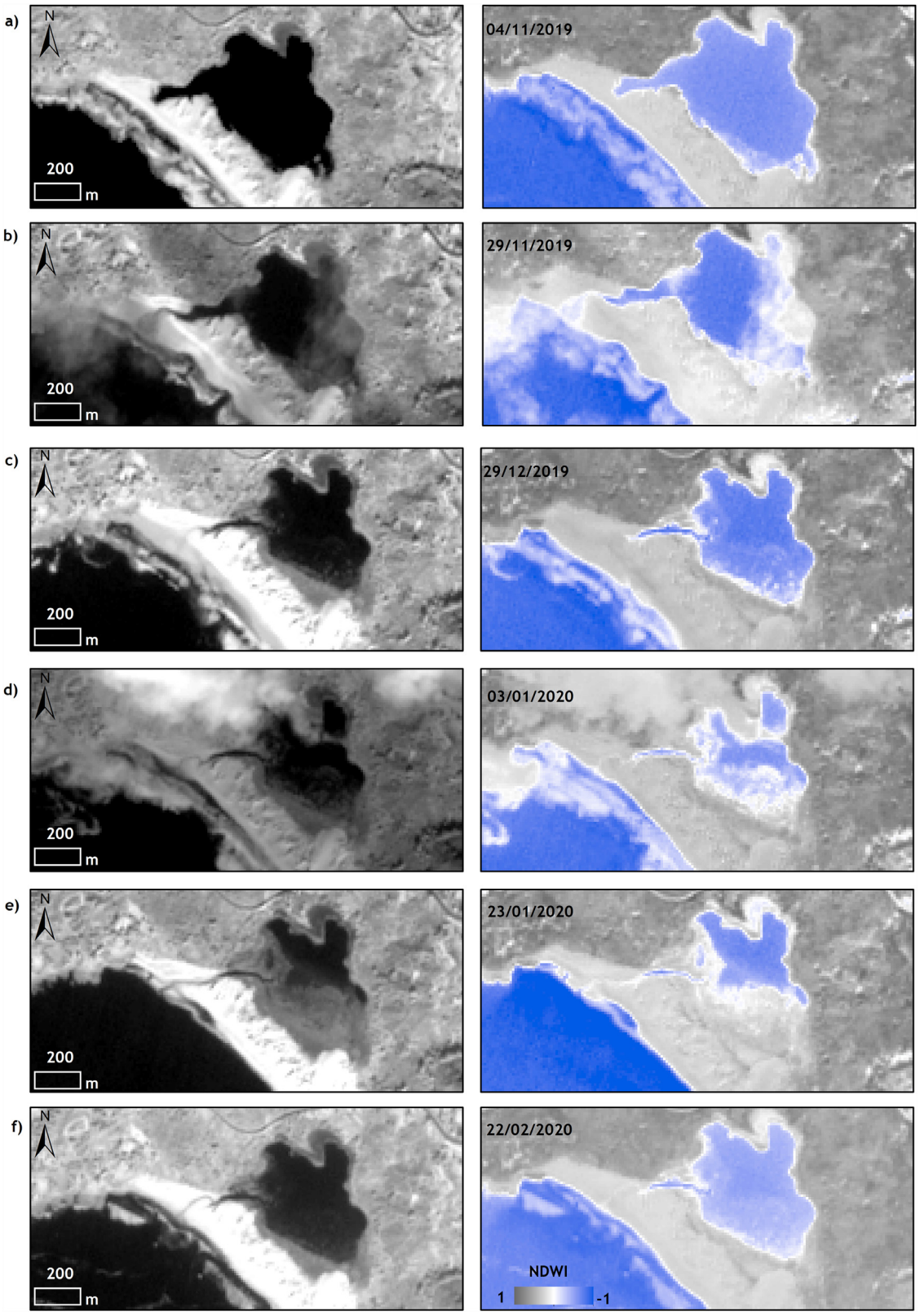

Figure 7 Example of the NDWI ($T \geq 0$) results compared to the NIR band (842 nm). Note that the Sentinel-2 images registered on 29/11/2019 and 03/01/2020 were both affected by clouds.

conventional in situ monitoring programmes providing continuous data in space and time. Although the breaking and closing of the sand barrier is a quick process that might happen within a timescale of a few days (Pérez-Arlucea et al., 2011), the number of available images (around two per month) was enough to reveal interesting information about these processes in combination with ancillary data. The availability of good quality images without cloud coverage affecting the lagoon determines the success of the methodology described in this study. Even though it was possible to have at least two images per month in the winter period, it is expected that summertime conditions increase the chance of having a higher number of good quality images that could allow a more detailed study.

Processing remote sensing images from digital levels (DN) or TOA values to surface reflectance is generally complicated. An accurate atmospheric correction needs input from many atmospheric variables such as aerosol concentration, optical depth or air pressure at sea level, as well as information about optically active constituents present in the water surface. Having data about all these parameters at the time of image acquisition is challenging (Du et al., 2002). Several studies have used DN or TOA, instead of surface reflectance to build water indices (Danaher et al., 2006; Donchyts et al., 2016; Ko et al., 2015), and obtained very similar results than when using surface reflectance (Fisher et al., 2016). In this study, TOA Sentinel-2 images provided a good delimitation of the lagoon water surface, and the results allowed the detection of the sand barrier break and the inlet. Two factors could explain why such a good delimitation from the data is possible. First, resizing the image to the Louro lagoon area remarkably reduces the pixel variability. Second, the arithmetic operation of the multiband water indices cancels out a large portion of noise (i.e. sensor calibration and changing radiation conditions caused by the illumination, soil, topography or atmospheric conditions) (Ji et al., 2009).

Although various comparative studies on multiband indices have been performed, no index was found to be effective in all scenarios (Boschetti et al., 2014). The Louro lagoon is located in a rural area with no significant terrain elevations around the lagoon. Both issues facilitate the delimitation of water bodies without interferences produced by urban areas or topographic shades. As expected, the spatial resolution of Sentinel-2 bands influenced the water surface delimitation, especially at the edges of the lagoon and the inlet. The NDVI and NDWI indices showed the best results regarding the water surface and inlet detection due to their higher spatial resolution bands (10 m). These results coincided with other studies where both indices were more efficient in extracting water bodies while removing most classification errors for shadow and other non-water surfaces (Acharya et al., 2018). The frequency density histograms analysis showed that the NDWI produced a better differentiation between water and terrestrial substrates (Figure 4). Thus, the NDWI was selected as the optimal index to monitor morphological and hydrological changes in the Louro lagoon. The discharge of water from the lagoon makes other substrates such as vegetation and sand appear (Fraga-Santiago et al., 2019). High reflection of vegetation and soil in NIR bands causes the NDWI to be less affected by this interaction at the lagoon edge and hence giving more accurate results. The lack of built-up classes adjacent to the water mass increases the accuracy of the NDWI, which generally cannot sufficiently suppress the reflectance from built-up areas. The selection of the NDWI as the optimal index was coincident with the results provided by Zhou et al. (2017). These authors (Zhou et al., 2017) compared several indices to map open surface water in the Poyang Lake Basin (China). Other studies also reported that the NDWI performs better in small lakes due to less interaction with classes adjacent to the water body (Özelkan, 2020).

One of the critical aspects of applying multiband water indices is the determination of an optimal threshold value. The optimal value can depend on the characteristics of each particular site and on the threshold method employed (Sekertekin, 2019). Due to the reflectance characteristics, the NDWI values for water are usually higher than zero. Therefore, a zero ($T \geq 0$) threshold is often applied to extract water from satellite images using this index. In the Louro lagoon, this threshold value showed a good delimitation of the water surface, including the inlet detection (Figure 7), except for the images registered on 29/11/2019 and 03/01/2020, due to the presence of clouds.

Employing the frequency histograms, populations of water, land and mixed pixels were identified. The number of mixed pixels is significant for coarse resolution satellite images (e.g. AVHRR (1 km), Sentinel-3 OLCI (300), MODIS (250 m)) where large pixels usually contain multiple types of substrates. Compared to these optical satellites, the spatial resolution of Sentinel-2 (10 m) reduces mixed pixels and their associated omission errors. For the purpose of this study, good results were obtained using a threshold value of $T \geq 0$. This threshold value ($T \geq 0$) accurately delimited submerged areas and was well suited to detect the sand barrier break and the inlet. The threshold value of $T \geq -0.1$ included mixed pixels that were interpreted as very shallow areas. It also showed a better delimitation of the inlet when the water flow is very low (e.g. Figure 1). However, new analyses of Sentinel-2 images, supported by field campaigns, will be necessary to better understand how the lagoonś water surface variations affect the selection of the optimal threshold value.

This study revealed that the lagoon suffers drastic water level variations during the opening and closing of the sand barrier. Even though field campaigns were not performed, the results related to the estimation of water surface coverage were very similar to those reported by other authors using different methodologies in the same study area (e.g. González-Villanueva et al., 2015). The results showed that the breaking and closing of the sand barrier could be a rapid process supporting the results obtained by Pérez-Arlucea et al. (2011). However, the water level can be recovered within less than one month. The sand barrier-breaking frequency and duration can drive different and complex effects on ecological, chemical and physical processes (Conde et al., 2015) and in many cases, these processes have not been explicitly evaluated yet (Yáñez-Aranciabia et al., 2014).

Sentinel-2 data could provide valuable information for establishing the sand barrier vulnerability frequency and preventing damage in these ecosystem services such as fisheries. For example, the breaking and closing of the sand bar-

rier of the Baldaio lagoon, a similar lagoon located on the Galician coast, has a direct impact on shellfish harvesting areas. The methodology proposed here could be transferred to similar sites for supporting coastal management.

Although the number of satellite applications in coastal lagoons has increased, the number of studies that include Sentinel-2 data is still small. Most of the Sentinel-2 applications are related to the assessment and monitoring of water quality parameters (e.g. Vaičiūtė et al., 2021), but the number of applications related to water body extraction is still scarce (e.g. Kaplan et al., 2017; Salameh et al., 2020). Due to the relatively short lifespan of Sentinel-2 mission (up to now 6 years), it is also common to find a combination of Sentinel-2 and Landsat data to study long term changes (e.g. Karim et al., 2019; Vaičiūtė et al., 2021). The series of Sentinel-2 data will increase in the future with the launch of Sentinel-2C and Sentinel-2D.

The vulnerability of the Louro lagoon and other similar lagoons will be enhanced in the coming decades due to climate change effects. Sea-level rise, intensification of storms, alteration in the tidal regimes, or changes in the freshwater inputs will have a substantial impact on the functioning of these areas. To prevent ecological losses and degradation due to climate change effects, continuous spatial and temporal information will be required. This study demonstrates the importance of Sentinel-2 data to monitor highly dynamic coastal areas such as coastal lagoons. The combination of Sentinel-2 data with in situ monitoring programmes will provide valuable information for coastal management that could contribute to face climate change effects and protect ecosystem services.

Declaration of competing interest

The authors declare that they have no known competing financial interests or personal relationships that could have appeared to influence the work reported in this paper.

Acknowledgements

The Copernicus programme, European Space Agency and European Commission are thanked for providing Sentinel-2 data. The author also thank Gloria Portilla for her assistance in the access to tide data and the two anonymous reviewers that, with their comments, helped to improve the initial version of this manuscript.

References

Acharya, T.D., Subedi, A., Lee, D.H., 2018. Evaluation of water indices for Surface Water Extraction in a Landsat 8 Scene of Nepal. Sensors 18, 2580. https://doi.org/10.3390/s18082580

Amécija, C, Villacieros-Robineau, N, Alejo, I, Pérez-Arlucea, M, et al., 2009. Morphodynamic conceptual model of an exposed beach: the case of Louro Beach (Galicia, NW Iberia). J. Coast Res. SI56 1711—1715.

Ansper, A., Alikas, K., 2019. Retrieval of chlorophyll a from Sentinel-2 MSI data for the European Union Water Framework Directive Reporting Purposes. Remote Sens 11 (1), 64. https://doi.org/10.3390/rs11010064

Bao, R., Alonso, A., Delgado, C., Pagés, J.L., 2007. Identification of the main driving mechanisms in the evolution of a small coastal wetland (Traba, Galicia, NW Spain) since its origin 5700 cal yr BP. Palaeogeogr. Palaeoclimatol. Palaeoecol. 247, 296—312. https://doi.org/10.1016/j.palaeo.2006.10.019

Barnes, R.S.K., 1980. Coastal Lagoons. Cambridge University Press, Cambridge, 106 pp.

Bertotti-Crippa, L., Stenert, C., Maltchik, L., 2013. Does the management of sandbar openings influence the macroinvertebrate communities in southern Brazil wetlands? A case study at Lagoa do Peixe National Park Ramsar site. Ocean Coastal Manage. 71, 26—32. https://doi.org/10.1016/j.ocecoaman.2012.10.009

Bird, E.C.F., 1994. Physical setting and geomorphology of coastal lagoons. In: Kjerfve, B. (Ed.), Coastal Lagoon Processes. Elsevier, Amsterdam, 9e39.

Boschetti, M., Nutini, F., Manfron, G., Brivio, P.A., Nelson, A., 2014. Comparative analysis of Normalised Difference Spectral Indices derived from MODIS for detecting surface water in flooded rice cropping systems. PLoS ONE 9 (2), e88741. https://doi.org/10.1371/journal.pone.0088741

Braga, F., Scarpa, G.M., Branco, V., Manfé, G., Zaggia, L., 2020. COVID-19 lockdown measures reveal human impact on water quality transparency in the Venice Lagoon. Sci. Total Environ. 736, 139612. https://doi.org/10.1016/j.scitotenv.2020.139612

Brisset, M., Van Wynsberge, S., Andréfouët, S., Payri, C., Soulard, B., Bourassin, E., Gendre, R.L., Coutures, E., 2021. Hindcast and Near Real-Time Monitoring of Green Macroalgae Blooms in Shallow Coral Reef Lagoons Using Sentinel-2: A New-Caledonia Case Study. Remote Sens. 13, 211. https://doi.org/10.3390/rs13020211

Bryant, R.G., Rainey, M.P., 2002. Investigation of flood inundation on playas within the Zone of Chotts, using a time-series of AVHRR. Remote Sens. Environ. 82, 360—375. https://doi.org/10.1016/S0034-4257(02)00053-6

Casal, G., Hedley, J.D., Monteys, X., Harris, P., Cahalane, C., McCarthy, T., 2020. Satellite-derived bathymetry in optically complex waters using a model inversion approach and Sentinel-2 data. Estuar. Coast. Shelf Sci. 241, 106814. https://doi.org/10.1016/j.ecss.2020.106814

Casal, G., Sánchez-Carnero, N., Sánchez-Rodríguez, E., Freire, J., 2011. Remote sensing with SPOT-4 for mapping kelp forest in turbid waters on the south European Atlantic shelf. Estuar. Coast. Shelf Sci. 91 (3), 371—378. https://doi.org/10.1016/j.ecss.2010.10.024

Conde, D., Vitancurt, J., Rodríguez-Gallego, L., de Álava, D., Verrastro, N., Chreties, C., Solari, S., Teixeira, L., Lagos, X., Piñeiro, G., Seijo, L., Caymaris, H., Panario, D., 2015. Solutions for Sustainable Coastal Lagoon Management: From Conflict to the Implementation of a Consensual Decision Tree for Artificial Opening. In: Baztan, J., Chouinard, O., Jorgensen, B., Tett, P., Vanderlinden, J.P., Vasseur, L. (Eds.), Coastal Zones. Solutions for the 21st Century. Elsevier, Amsterdam, The Netherlands, 217—250.

Costas, S., Muñoz-Sobrino, C., Alejo, I., Pérez-Arlucea, M., 2009. Holocene evolution of a rock-bounded barrier-lagoon system. Cíes Islands, northwest Iberia, Earth Surf. Proc. Land 34, 1575—1586. https://doi.org/10.1002/esp.1849

Danaher, T., Collett, L., 2006. Development, optimisation and multi-temporal application of a simple Landsat based water index. Paper presented at 13th Australasian Remote Sensing and Photogrammetry Conference, Canberra, Australia, 21—22 November 2006.

Davies, J.L., 1964. A morphogenetic approach to world shorelines. Zeitschrift fur Geomorphology 8, 127—142.

DeVries, B., Huang, C., Armston, J., Huang, W., Jones, J.W., Lang, M.W., 2020. Rapid and robust monitoring of flood events

using Sentinel-1 and Landsat data on the Google Earth Engine. Remote Sens. Environ. 240, 111664. https://doi.org/10.1016/j.rse.2020.111664

Donchyts, G., Schellekens, J., Winsemius, H., Eisemann, E., van de Giesen, N., 2016. A 30 m resolution surface water mask including estimation of positional and thematic differences using Landsat 8, SRTM and OpenStreetMap: A case study in the Murray-Darling Basin, Australia. Remote Sens. 8 (5), 386. https://doi.org/10.3390/rs8050386

Du, Y., Teillet, P.M., Cihlar, J., 2002. Radiometric normalisation of multitemporal high-resolution satellite images with quality control for land cover change detection. Remote Sens. Environ. 82 (1), 123—134. https://doi.org/10.1016/S0034-4257(02)00029-9

Du, Y., Zhan, Y., Ling, F., Wang, Q., Li, W., Li, X., 2016. Water bodies'mapping from Sentinel-2 imagery with Modified Normalized Difference Water Index at 10-m spatial resolution produced by sharpening the SWIR band. Remote Sens. 8 (4), 354. https://doi.org/10.3390/rs8040354

Du, Z., Linghu, B., Ling, F., Li, W., Tian, W., Wang, H., Gui, Y., Sun, B., Zhang, X., 2012. Estimating surface water area changes using time-series Landsat data in the Qingjiang River Basin. China. J. Appl. Remote Sens. 6, 063609. https://doi.org/10.1117/1.JRS.6.063609

Duan, Z., Bastiaanssen, W.G.M., 2013. Estimating water volume variations in lakes and reservoirs from four operational satellite altimetry databases and satellite imagery data. Remote Sens. Environ. 134, 403—416. https://doi.org/10.1016/j.rse.2013.03.010

Duck, R.W., Figueiredo da Silva, J., 2012. Coastal lagoons and their evolution: A hydromorphological perspective. Estuar. Coast. Shelf. 110, 2—14. https://doi.org/10.1016/j.ecss.2012.03.007

EC, 1992. Council Directive 92/43/EEC of 21 May 1992 on the conservation of natural habitats and of wild fauna and flora. Official Journal L 206, 7—50. https://eur-lex.europa.eu/LexUriServ/LexUriServ.do?uri=CELEX:31992L0043:EN:HTML

EC, 2000. Directive 2000/60/EC of the European Parliament and of the Council of 23 October 2000 establishing a framework for Community action in the field of water policy. Official Journal L 327, 0001—0073, 22/12/2000 P. https://eur-lex.europa.eu/eli/dir/2000/60/oj

Feyisa, G.L., Meilby, H., Fensholt, R, Proud, S.R., 2014. Automated water extraction index: A new technique for surface water mapping using Landsat imagery. Remote Sens. Environ. 140, 23—35. https://doi.org/10.1016/j.rse.2013.08.029

Fisher, A., Flood, N., Danaher, T., 2016. Comparing Landsat water index methods for automated water classification in eastern Australia. Remote Sens. Environ. 175, 167—182. https://doi.org/10.1016/j.rse.2015.12.055

Fortunato, A.B., Nahon, A., Dodet, G., Pires, A.R., Freitas, M.C., Bruneau, N., Azevedo, A., Bertin, X., Benevides, P., Andrade, C., Oliveira, A., 2014. Morphological evolution of an ephemeral tidal inlet from opening to closure: the Albufeira inlet, Portugal. Cont. Shelf Res. 73 (1), 49—63. https://doi.org/10.1016/j.csr.2013.11.005

Fraga-Santiago, P., Gómez-Pazo, A., Pérez-Alberti, A., Montero, P., Otero-Pérez, A., 2019. Trends in the recent evolution of coastal lagoons and lakes in Galicia (NW Iberian Peninsula). J. Mar. Sci. Eng. 7, 272. https://doi.org/10.3390/jmse7080272

Frazier, P.S., Page, K.J., 2000. Water body detection and delineation with Landsat TM data. Photogramm. Eng. Remote Sens. 66 (12), 1461—1467.

Gale, E., Pattiaratchi, C., Ranasinghe, R., 2006. Vertical mixing processes in intermittently closed and open lakes and lagoons, and the dissolved oxygen response. Estuar. Coast. Shelf Sci. 69 (1—2), 205—216. https://doi.org/10.1016/j.ecss.2006.04.013

Gholizadeh, M.H., Melesse, A.M., Reddi, L., 2016. A comprehensive review on water quality parameters estimation using remote sensing techniques. Sensors 16 (8), 1298. https://doi.org/10.3390/s16081298

González-Villanueva, R., Costas, S., Pérez-Arlucea, M., Jerez, S., Trigo, R.M., 2013. Impact of atmospheric circulation patterns on coastal dune dynamics, NW Spain. Geomorphology 185, 96—109. https://doi.org/10.1016/j.geomorph.2012.12.019

González-Villanueva, R., Pérez-Arlucea, M., Costas, S., 2017. Lagoon water-level oscillations driven by rainfall and wave climate. Coast. Eng. 130, 34—45. https://doi.org/10.1016/j.coastaleng.2017.09.013

González-Villanueva, R., Pérez-Arlucea, M., Costas, S., Bao, R., Otero, X.L., Goble, R., 2015. 8000 years of environmental evolution of barrier—lagoon systems emplaced in coastal embayments (NW Iberia). The Holocene 25 (11), 1786—1801. https://doi.org/10.1177/0959683615591351

Green, A., Cooper, J.A.G., LeVieux, A., 2013. Unusual barrier/inlet behaviour associated with active coastal progradation and river-dominated estuaries. J. Coast. Res. 35—45. https://doi.org/10.2112/SI_69_4

Guo, Y.L., Li, Y.M., Zhu, L., Liu, G, Wang, S, Du, C.G., 2015. An Improved Unmixing-Based Fusion Method: Potential application to remote monitoring of inland waters. Remote Sens. 7, 1640—1666. https://doi.org/10.3390/rs70201640

Hedley, J.D., Roelfsema, C., Brando, V., Giardino, C., Kutser, T., Phinn, S., Mumby, P.J., Barrilero, O., Laporte, J., Koetz, B., 2018. Coral reef applications of Sentinel-2: Coverage, characteristics, bathymetry and benthic mapping with comparison to Landsat 8. Remote Sens. Environ. 216, 598—614. https://doi.org/10.1016/j.rse.2018.074

Ji, L., Zhang, L., Wylie, B., 2009. Analysis of dynamic thresholds for the normalised difference water index. Photogramm. Eng. Remote Sens. 75 (11), 1307. https://doi.org/10.14358/PERS.75.11.1307

Kaplan, G., Avdan, U., 2017. Object-based water body extraction model using Sentinel-2 satellite imagery. Int. J. Remote Sens. 50 (1), 1297540. https://doi.org/10.1080/22797254.2017.1297540

Karim, M., Maanan, M., Maanan, M., Rhinane, H., Rueff, H., Baidder, L., 2019. Assessment of water body change and sedimentation rate in Moulay Bousselham wetland, Morocco, using geospatial technologies. Int. J. Sediment Res. 34, 65—72. https://doi.org/10.1016/j.ijsrc.2018.08.007

Kjerfve, B., 1994. In: Kjerfve, B. (Ed.). Coastal Lagoon Processes, Amsterdam, 1—8.

Ko, B., Kim, H., Nam, J., 2015. Classification of potential water bodies using Landsat 8 OLI and a combination of two boosted Random Forest classifiers. Sensors 15 (6), 13763. https://doi.org/10.3390/s150613763

Lavery, P., Pattiaratchi, C., Wyllie, A., Hick, P., 1993. Water quality monitoring in estuarine waters using the Landsat thematic mapper. Remote Sens. Environ. 46 (3), 268—280. https://doi.org/10.1016/0034-4257(93)90047-2

Li, W., Du, Z., Ling, F., Zhou, D., Wang, H., Gui, Y., Sun, B., Zhang, X.A., 2013. A comparison of land surface water mapping using the normalised difference water index from TM, ETM+ and ALI. Remote Sens. 5 (11), 5530—5549. https://doi.org/10.3390/rs5115530

Liu, X., Deng, R., Xu, J., Zhang, F., 2017. Coupling the modified linear spectral mixture analysis and pixel-swapping methods for improving subpixel water mapping: application to the Pearl River Delta, China. Water 9 (9), 658. https://doi.org/10.3390/w9090658

Luis, K.M.A., Rheuban, J.E., Kavanaugh, M.T., Glover, D.M., Wei, J., Lee, Z., Doney, S.C., 2019. Capturing coastal water clarity variability with Landsat 8. Mar. Pollut. Bull. 145, 96—104.

McFeeters, S.K., 1996. The use of the Normalised Difference Water Index (NDWI) in the delineation of open water features. Int. J. Remote Sens. 17, 1425—1432. https://doi.org/10.1080/01431160600589179

Meng, W., Zhu, S., Cao, W., Su, X., Cao, B., 2013. Establishment of synthetical water index. Science of Surveying and Mapping 38 (4), 130—133.

Moreno, I.M., Avila, A., Losada, M.A., 2010. Morphodynamics of intermittent coastal lagoons in southern Spain: Zahara de los atunes. Geomorphology 121 (3—4), 305—316. https://doi.org/10.1016/j.geomorph.2010.04.028

Newton, A., Brito, A.C., Icely, J.D., Derolez, V., Clara, I., Angus, S., Schernewski, G., Inácio, M., Lillebø, A.I., Sousa, A.I., Béjaoui, B., Solidoro, C., Tosic, M., Cañedo-Argüelles, M., Yamamuro, M., Reizopoulou, S., Tseng, H.C., Canu, D., Roselli, L., Maanan, M., Cristina, S., Ruiz-Fernández, A.C., Lima, R.F.D., Kjerfve, B., Rubio-Cisneros, N., Pérez-Ruzafa, A., Marcos, C., Pastres, R., Pranovi, F., Snoussi, M., Turpie, J., Tuchkovenko, Y., Dyack, B., Brookes, J., Povilanskas, J.R., Khokhlov, V., 2018. Assessing, quantifying and valuing the ecosystem services of coastal lagoons. J. Nat. Conserv. 44, 50—65. https://doi.org/10.1016/j.jnc.2018.02.009

Özelkan, E., 2020. Water body detection analysis using NDWI indices derived from Landsat-8 OLI. Pol. J. Environ. Stud. 29 (2), 1759—1769. https://doi.org/10.15244/pjoes/110447

Pérez-Arlucea, M., Almecija, C., González-Villanueva, R., Alejo, I., 2011. Water dynamics in a barrier-lagoon system: controlling factors. J. Coast. Res. SI 64, 15—19.

Rokni, K., Ahmad, A., Selamat, A., Hazini, S., 2014. Water feature extraction and change detection using multitemporal Landsat Imagery. Remote Sens. 6, 4173—4189. https://doi.org/10.3390/rs6054173

Rouse, J.W., Haas, R.H, Schell, J.A., Deering, D.W., 1973. Monitoring vegetation systems in the Great Plains with ERTS (Earth Resources Technology Satellite). In: Proceedings of the Third Earth Resources Technology Satellite Symposium, Greenbelt, ON, Canada, 10—14 December, 309—317.

Salameh, E., Frappart, F., Turki, I., Laignen, B., 2020. Intertidal topography using the waterline method from Sentinel-1 and Sentinel-2 images: the examples of Arcachon and Veys Bays in France. ISPRS J. Photogramm. Remote Sens. 163, 98—120. https://doi.org/10.1016/j.isprsjprs.2020.03.003

Sebastiá-Frasquet, M.T., Aguilar-Maldonado, J.A., Santamaría-del-Ángel, E., Estornell, J., 2019. Sentinel 2 analysis of turbidity patterns in a coastal lagoon. Remote Sens. 11 (24), 2926. https://doi.org/10.3390/rs11242926

Sekertekin, A., 2019. Potential of global thresholding methods for the identification of surface water resources using Sentinel-2 satellite imagery and normalised difference water index. J. Appl. Remote Sens. 13 (4), 044507. https://doi.org/10.1117/1.JRS.13.044507

Smakhtin, V. , 2004. Simulating the hydrology and mouth conditions of small, temporarily closed/open estuaries. Wetlands 24, 123—132. https://doi.org/10.1672/0277-5212(2004)024[0123:STHAMC]2.0.CO;2

Sòria-Perpinyà, X., Vicente, E., Urrego, P., Pereira-Sandoval, M., Ruíz-Verdú, A., Delegido, J., Soria, J.M., Moreno, J., 2020. Remote sensing of cyanobacterial blooms in a hypertrophic lagoon (Albufera of Valencia, Eastern Iberian Peninsula) using multitemporal Sentinel-2 images. Sci. Total Environ. 698, 123305. https://doi.org/10.1016/j.scitotenv.2019.134305

Sun, F., Sun, F., Chen, J., Gong, P., 2012. Comparison and improvement of methods for identifying waterbodies in remotely sensed imagery. Int. J. Remote Sens. 33, 6854—6875. https://doi.org/10.1080/01431161.2012.692829

Tagliapietra, D., Sigovini, M., Ghirardini, A.V., 2009. A review of terms and definitions to categorise estuaries, lagoons and associated environments. Mar. Freshw. Res. 60, 497e509. https://doi.org/10.1071/MF08088

Vaičiūtė, D., Bučas, M., Bresciani, M., Dabulevičienė, T., Gintauskas, J., Mėžinė, J., Tiškus, E., Umgiesser, G., Morkūnas, J., De Santi, F., Bartoli, M., 2021. Hot moments and Hotspots of cyanobacteria hyperblooms in the Curonian Lagoon (SE Baltic Sea) revealed via remote sensing-based retrospective analysis. Sci. Total Environ. 769, 145053. https://doi.org/10.1016/j.scitotenv.2021.145053

Wang, Z., Liu, J., Li, J., Zhang, D.V., 2018. Multi-Spectral Water Index (MuWI): A native 10-m multi-spectral water index for accurate water mapping on Sentinel-2. Remote Sens. 10 (10), 1643. https://doi.org/10.3390/rs10101643

Weidman, C.R., Ebert, J.R., 2013. In: Aubrey, D.G., Giese, G.S. (Eds.), Cyclic Spit Morphology in a Developing Inlet System, 44. American Geophysical Union, Washington DC, 186—212.

Xie, H., Luo, X., Xu, X., Tong, X., Jin, Y., Pan, H., Tong, X., 2014. New hyperspectral difference water index for the extraction of urban water bodies by the use of airborne hyperspectral images. J. Appl. Remote Sens. 8, 5230—5237. https://doi.org/10.1117/1.JRS.8.085098

Xu, H., 2005. A study on information extraction of water body with the modified normalised difference water index (MNDWI). Int. J. Remote Sens. 9 (5), 589—595. https://doi.org/10.1080/01431160600589179

Xu, H., 2006. Modification of normalised difference water index (NDWI) to enhance open water features in remotely sensed imagery. Int. J. Remote Sens. 27, 3025—3033. https://doi.org/10.1080/01431160600589179

Yang, X., Zhao, S., Qin, X., Zhao, N., Liang, L., 2017. Mapping of urban surface water bodies from Sentinel-2 MSI imagery at 10 m resolution via NDWI-based image sharpening. Remote Sens. 9 (6), 596. https://doi.org/10.3390/rs9060596

Yáñez-Aranciabia, A., Day, J.W., Sánchez-Gil, P., Day, J.N., Lane, R.R., Zárate-Lomelíc, D., Alafita-Vásquez, H., Rojas-Galaviz, J.L., Ramírez-Gordillo, J., 2014. Ecosystems functioning: the basis for restoration and management of a tropical coastal lagoon, Pacific coast of Mexico. Ecol. Eng. 65, 88—100. https://doi.org/10.1016/j.ecoleng.2013.03.007

Zhang, F., Li, J., Zhang, B., Shen, Q., Ye, H., Wang, S., Lu, Z., 2018. A simple automated dynamic threshold extraction method for the classification of large water bodies from Landsat-8 OLI water index images. Int. J. Remote Sens. 39 (11), 3429—3451. https://doi.org/10.1080/01431161.2018.1444292

Zhang, T., Yang, X., Hu, S., Su, F., 2013. Extraction of coastline in aquaculture coast from multispectral remote sensing images: object-based region growing integrating edge detection. Remote Sens. 5 (9), 4470—4487. https://doi.org/10.3390/rs5094470

Zhou, Y., Dong, J., Xiao, X., Xiao, T., Yang, Z., Zhao, G., Zou, Z., Qin, Y., 2017. Open surface water mapping algorithms: a comparison of water-related spectral indices and sensors. Water 9 (4), 256. https://doi.org/10.3390/w9040256